ARMA 19-040

SAND2019-1939C

Shear Behavior of Bedded Salt Interfaces and Clay Seams

Sobolik, S.R. [1*], S.A. Buchholz [2], E. Keffeler[2], S. Borglum[2], B. Reedlunn [1]

[1] *Sandia National Laboratories, Albuquerque, New Mexico, USA;* [2] *RESPEC, Rapid City, South Dakota, USA*

ABSTRACT: Bedded salt contains interfaces between the host salt and other in situ materials such as clay seams, or different materials such as anhydrite or polyhalite in contact with the salt. These inhomogeneities are thought to have first-order effects on the closure of nearby drifts and potential roof collapses. Despite their importance, characterizations of the peak shear strength and residual shear strength of interfaces in salt are extremely rare in the published literature. This paper presents results from laboratory experiments designed to measure the mechanical behavior of a bedding interface or clay seam as it is sheared. The series of laboratory direct shear tests reported in this paper were performed on several samples of materials from the Permian Basin in New Mexico. These tests were conducted at several normal and shear loads up to the expected in situ pre-mining stress conditions. Tests were performed on samples with a halite/clay contact, a halite/anhydrite contact, a halite/polyhalite contact, and on plain salt samples without an interface for comparison. Intact shear strength values were determined for all of the test samples along with residual values for the majority of the tests. The test results indicated only a minor variation in shear strength, at a given normal stress, across all samples. This result was surprising because sliding along clay seams is regularly observed in the underground, suggesting the clay seam interfaces should be weaker than plain salt. Post-test inspections of these samples noted that salt crystals were intrinsic to the structure of the seam, which probably increased the shear strength as compared to a more typical clay seam.

1. INTRODUCTION

Extensive collaborations between American and German salt repository researchers have identified four key research areas to better understand the behavior of salt for radioactive waste repositories (Hansen et al., 2016a, 2016b and 2017). One subject area includes the influence of inhomogeneities. No in situ characterization testing has been published, yet inhomogeneities are thought to have first-order effects on excavation behavior. Included among these inhomogeneities are clay seams in bedded salt, or other interfaces such as halite/anhydrite and halite/polyhalite. These interfaces are prevalent in bedded salt formations such as in the Delaware Basin where the Waste Isolation Pilot Plant (WIPP) resides near Carlsbad, New Mexico, USA.

An idealized WIPP stratigraphy used for rock mechanics calculations with many interfaces is illustrated in Figure 1. The effects of shear along these interfaces have long been thought to have significant impacts on the mechanical behavior of disposal rooms built for the long-term disposal of radioactive waste, particularly as they pertain to the evolution of room closure, roof falls, and changes in strength and permeability at these interfaces. Figure 2 shows a photograph looking into a vertical borehole at WIPP, where three interfaces have clearly slid since the borehole was originally drilled.

There are essentially no published in situ measurement data for bedded salt deposits characterizing shear strength of an interface in salt and resulting effects of interface displacement and permeability. Munson and Matalucci (1983) proposed an in situ test for the WIPP site, with direct shear across a clay seam. A 1-by-1-m block in a wall containing a representative clay seam was to be isolated by cutting around it. Flatjacks were to be installed in slots cut around the block to apply shear and normal stresses. Displacements along and across the seam would be measured as a function of applied stress. This proposed test never occurred.

Some laboratory investigations have evaluated the slip along interfaces under several different stress environments. Minkley and Mühlbauer (2007) documented direct shear laboratory tests on carnallite and salt blocks under varying normal and shear loads and shear velocities. With these data, they developed a shear model for interfaces that accounts for both velocity-dependent and displacement-dependent shear softening mechanisms. The plots in Figure 3, taken from Minkley and Mühlbauer (2007), show the evolution of shear stress as a function of shear displacement for two different shear velocities. Their results showed that under higher shear velocities, adhesive frictional resistance must first be

Sandia National Laboratories is a multimission laboratory managed and operated by National Technology & Engineering Solutions of Sandia, LLC, a wholly owned subsidiary of Honeywell International Inc., for the U.S. Department of Energy's National Nuclear Security Administration under contract DE-NA0003525.

exceeded before a loss of shear strength occurs; at lower shear velocities, no adhesion is apparent, and cohesion is maintained.

WIPP contains halite/clay/halite, halite/anhydrite, and halite/polyhalite interfaces, not halite/carnallite interfaces, so the Minkley and Mühlbauer (2007) results are not directly applicable. In the absence of experimental data, the clay seams at WIPP have been modeled using Coulomb friction with an assumed friction coefficient of 0.2, while the other interfaces have been assumed to be perfectly bonded with infinite strength. Clearly, it would be preferable to have interface models based on laboratory tests for WIPP performance assessment simulations.

The series of laboratory direct shear tests reported in this paper were designed to measure, evaluate, and quantify the effects of shear displacement along a bedding interface or clay seam on shear and fracture strength of the interface and accompanying salt (Buchholz, 2019). These lab tests will be used to develop constitutive models for sliding and fracturing along bedding interfaces and clay seams at WIPP. In addition to applications directly related to WIPP, the data from these tests will be used to support US-German collaborative model development efforts for Joint Project WEIMOS (2016 – 2019; "Further Development and Qualification of the Rock Mechanical Modeling for the Final HAW Disposal in Rock Salt") (Lüdeling et al., 2018).

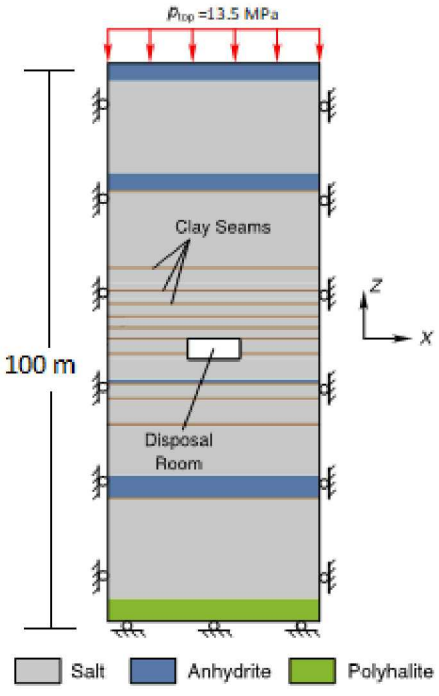

Fig. 1. Idealized WIPP stratigraphy.

Fig. 2. Example of interface sliding in a borehole at WIPP.

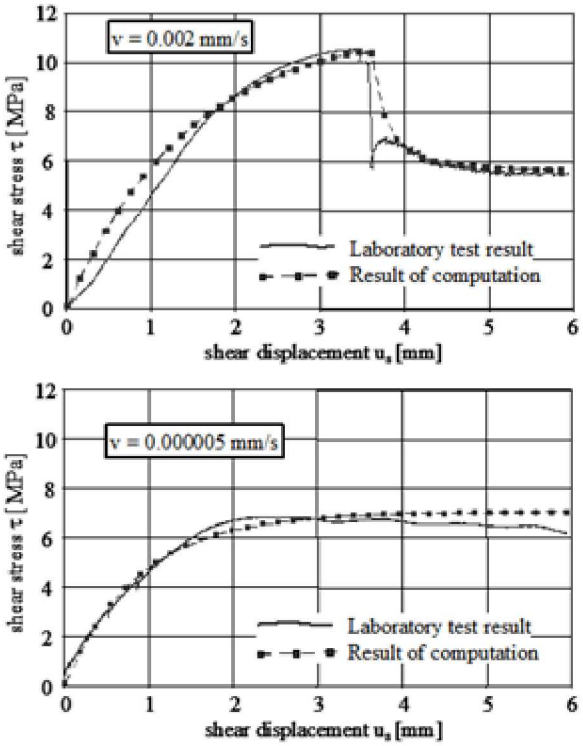

Fig. 3. Shear stress vs. displacement for different shear velocities (Minkley and Mühlbauer, 2007).

2. EXPERIMENTAL PROCEDURE

A series of laboratory direct shear tests was performed on several samples of materials assumed to be typical of WIPP emplacement rooms. These tests were conducted at several normal and shear loads up to expected in situ pre-mining stress conditions, and at a single shear velocity of 0.01 in/min (0.0042 mm/sec). This shear velocity is currently the slowest capable on this direct shear machine, so these tests were unable to evaluate potential velocity-dependent shear stress evolution. The direct shear test method was designed to measure the

complete shear stress-strain curve and characterize the following mechanical properties:

- Intact normal and shear stiffness
- Dependence of shear yield, ultimate, and residual strength on normal stress
- Residual normal and shear stiffness

Ultimate strength was the maximum shear stress measured during the test. Residual strength corresponds to the shear stress when the specimen shows perfectly plastic shear deformation behavior and was chosen as the lowest value of shear stress after decreasing to a nominally constant value. The test program followed three distinct phases, each of which is covered in the following subsections:

1. Extraction of test core with a clay seam, a halite/anhydrite interface, a halite/polyhalite interface, or plain salt (control specimens). Two types of plain salt were obtained: a "pure" salt with minimal visible impurity content, and "mixed" salt with more obvious impurity content.
2. Experiment preparation, including test sample preparation and setup of the direct shear machine.
3. Perform a suite of direct shear tests on 30 specimens, varying the normal stresses.

The project's test plan (Sobolik, 2017) includes further details of specimen preparation, test setup, multi-stage shear tests, and data processing.

2.1. Test core extraction

Sample collection was conducted in a salt-potash mine located near the WIPP facility. According to the original plan, as many samples as possible were to be drilled from the floor of an inclined drift at the mine. An exposed seam in the rib (side wall) of the drift would be followed until it went into the inclined floor. Core was to be extracted from a location where the interface was estimated to be approximately 24 inches (60 cm) below the floor. Several sites along the drift of the mine were scouted for well-defined clay seams, or well-defined interfaces between halite and another material (anhydrite or polyhalite). Two such locations are shown in Figure 4.

The cores were drilled using a concrete coring rig with a diamond bit core barrel having dimensions of 12 inches (300 mm) in diameter and 22 inches (560 mm) long. Several cores were drilled from the floor as planned, but nearly all exhibited damaged seams or interfaces, which made them unsuitable for testing. As a result, a determination was made to extract cores horizontally from the rib. This procedure was much more successful; several intact cores were extracted for all the desired interface types. The extraction of two such cores are illustrated in Figure 5. These cores were wrapped in plastic wrap and bubble wrap after extraction to maintain in situ moisture content.

In addition to the cores obtained from the mine, RESPEC obtained sections of nominally 4-inch (102-mm) diameter core from a Prairie Evaporite storage well in Alberta, Canada. These samples were used for the initial tests to qualify the test conditions and procedures.

Fig. 4. Exposed Clay Seam (Top) and Halite/Polyhalite Contact (Bottom) for Test Core Collection (regions in photos are approximately 6 feet wide).

Fig. 5. Core extraction from side wall of drift.

2.2. *Specimen preparation*

Four-inch (10-cm) diameter cylindrical specimens were subcored from the field core using a vertical mill. Bright-Cut NHG metal working fluid was used as a lubricant during subcoring to prevent washing of the evaporite materials. The long axes of the subcores were oriented perpendicular to the geologic interface to the extent possible. The subcores were trimmed so that the specimen length on either side of the interface was between 2 and 3 inches (5 and 7.6 cm). Total specimen length did not exceed 6 inches (15.2 cm). The specimens were then cleaned using an alcohol-based degreaser.

A 4-inch diameter cylindrical specimen was the largest size that the direct shear machine could apply the required stresses to. Resistance to sliding along an interface increases with specimen size because the likelihood of geometric locking of undulations and asperities increases. Interfaces contain mean undulation spacings on multiple length scales, ranging from microscopic spacings to hundreds of foot spacings. The 4-inch diameter specimens contained undulations on the order of an inch (2.5 cm), but obviously did not capture larger undulations, so the behavior measured herein should provide a lower bound on the interface residual shear strengths.

The specimens were photographed, and the diameter d of each specimen was measured at the interface (see Table 1) in order to calculate the undeformed cross-sectional area A_0. The specimens were coated with a clear, spray acrylic to protect the salt from possible dissolution by the grout. After the acrylic coatings cured, the test specimens were encapsulated in shear boxes using quick-curing, gypsum cement anchor grout, and the grout cured overnight. Not all specimens had interfaces that were parallel to the top and bottom of the cylinder; some specimens had to be oriented, or tilted, during the grouting process so that the interface ran parallel to and was centered in the gap between the shear boxes and aligned with the shear ram. This tilt angle for each specimen is noted in Table 1. The inside surfaces of the shear boxes are nominally 7 inches (18 cm) square, and the inner height of each box is 3 inches (7.5 cm). To prevent damage to the interface, clamps held the top and bottom portions of the shear boxes together until the shear box assembly was mounted in the shear testing machine.

All of the tested specimens have a unique identification number for tracking within the RESPEC laboratory. Depending on their provenance, specimens have one of two identification numbers:

- CANADA/HALITE-CLAY/506.07, where
  - Canada = regional location
  - Halite-Clay = specimen type
  - 506.07 = well depth (meters)
- CARLSBAD/HALITE-CLAY/1/1.45, where
  - Carlsbad = regional location
  - Halite-Clay = specimen type
  - 1 = specimen piece number
  - 1.45 = depth from wall (inches)

Table 1. Specimens tested.

Specimen I.D.	Avg. Diam. (in)	Tilt Angle (□)
CANADA/HALITE-CLAY/506.07	3.92	7
CANADA/HALITE-CLAY/507.28	3.87	3
CANADA/HALITE-CLAY/507.90	3.93	5
CANADA/HALITE-CLAY/506.84	3.87	2
CARLSBAD/HALITE-CLAY/1/1.45	3.99	3
CARLSBAD/HALITE-CLAY/3/1.00	4.00	0
CARLSBAD/HALITE-CLAY/2/1.15	4.00	7
CARLSBAD/HALITE-CLAY/3/0.80	4.00	4
CARLSBAD/HALITE-CLAY/6/0.80	4.00	0
CARLSBAD/POLYHALITE-HALITE/5/0.64	4.00	4
CARLSBAD/POLYHALITE-HALITE/1/0.10	3.99	8
CARLSBAD/POLYHALITE-HALITE/6/1.92	4.00	13
CARLSBAD/POLYHALITE-HALITE/4/0.64	4.00	15
CARLSBAD/POLYHALITE-HALITE/4/1.59	4.00	7
CARLSBAD/POLYHALITE-HALITE/3/1.59	4.00	5
CARLSBAD/MIXED-HALITE/1/1.76	4.00	0
CARLSBAD/MIXED-HALITE/3/1.00	3.99	0
CARLSBAD/MIXED-HALITE/2/1.76	4.00	0
CARLSBAD/MIXED-HALITE/4/1.76	4.00	0
CARLSBAD/MIXED-HALITE/5/1.76	3.99	0
CARLSBAD/PURE-HALITE/6/0.68	3.99	0
CARLSBAD/PURE-HALITE/1/0.00	3.99	0
CARLSBAD/PURE-HALITE/2/0.00	3.99	0
CARLSBAD/PURE-HALITE/8/0.68	3.99	0
CARLSBAD/PURE-HALITE/10/0.68	3.99	0
CARLSBAD/HALITE-ANHYDRITE/2/1.90	4.00	4
CARLSBAD/HALITE-ANHYDRITE/1/0.22	3.99	3
CARLSBAD/HALITE-ANHYDRITE/3/2.30	3.99	7
CARLSBAD/HALITE-ANHYDRITE/1/2.30	4.00	8
CARLSBAD/HALITE-ANHYDRITE/1/1.41	4.00	12

2.3. *Test equipment*

Normal stresses of 1,000–2,400 psi (7–17 MPa) were required to approximate in situ overburden stress conditions at WIPP (approximately 15 MPa). For this reason, the RESPEC direct shear machine, shown in Figure 6, was selected to perform the tests because it has an axial and shear load capacity of 30,000 pounds (130 kN) each, which meets the 2,400 psi (17 MPa) requirement for the 4-inch- (100-mm-) diameter cylinders. Potentiometric linear displacement sensors were mounted on the shear boxes to measure shear displacement. Load cells on the machine measured the normal load P and shear load S applied to the seam or interface. The shear displacement was applied to the top block, while the bottom block was held fixed.

The direct shear machine's stiffness to loads normal to the shear plane was measured using a solid steel specimen prepared using the same procedure for preparing a salt specimen, including the grout between the specimen and the shear box. Plots of the normal stress P/A_0 versus normal displacement showed that loading to less than 600 psi (4 MPa) resulted in a non-linear response during

reloading. When normal loading exceeded 600 psi, the reload response was linear and a normal stiffness could be measured from the reloading response. Thus, the normal stiffness was only calculated for the tests run at a normal stress greater than 600 psi (4 MPa). The average normal stiffness calculated from the slope of the load-unload-reload cycles on the steel specimens was approximately 250,000 psi/in (67.9 MPa/mm). Normal stiffness values calculated for the rock specimens that exceeded the value for the steel specimen were deemed invalid.

The normal stiffness of the test setup depends on several factors including machine components, the encapsulating grout, and the interfaces between the grout and shear boxes. The factors related to encapsulation grout are not always consistent between specimens. When testing of soft clay interfaces, inconsistencies between the test setups for each specimen are second order and do not have a significant effect on the measured normal stiffness of the specimens. However, the specimens tested for this project had stiff interfaces, and for these specimens the non-reproducibility in test setup had more significant effects on measured normal stiffness. Consequently, the reported normal stiffness values should be regarded as estimates.

The machine's stiffness to shear loading was also measured, but not reported here. Although the shear displacement transducer was appropriate for measuring the gross motion during the tests, its precision was insufficient for measuring shear stiffnesses of these stiff specimens.

The load cells and linear displacement sensors were calibrated to standards traceable to the National Institute of Standards and Technology (NIST).

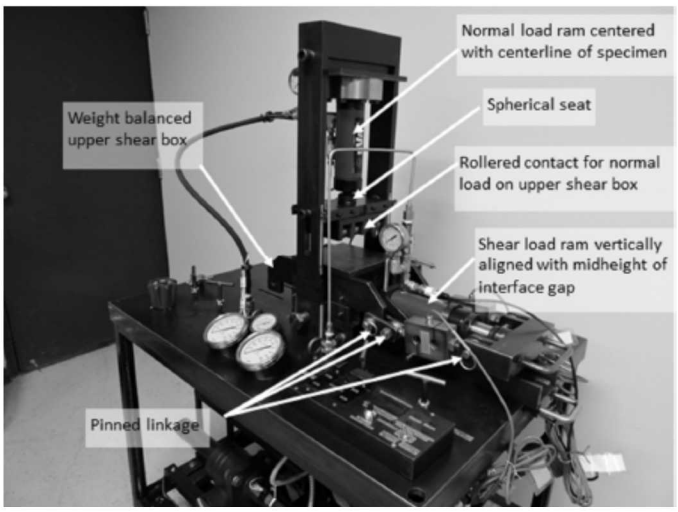

Fig. 6. RESPEC direct shear machine and test setup.

2.4. *Test procedure*

The shear test procedure began with a load-unload-reload cycle of the normal stress. The cycle consisted of loading to the target normal stress specified for that specimen, unloading to approximately P/A_0 = 200 psi (1.4 MPa), then reloading to the target normal stress. The initial loading reduced the compliance of the shear box assembly in the normal loading direction so that the intact normal stiffness could be calculated from the reload portion of the cycle. No damage to the samples was observed during this step. After completing the normal stress load-unload-reload cycle, the target normal stress on the specimen P/A_0 remained constant through the remainder of the shear test. The four target normal stresses were P/A_0 = 500, 1000, 1500, and 2400 psi (3.4, 6.9, 10.3, and 16.5 MPa). At least one specimen of each specimen type was loaded to each target normal stress.

Once the normal stress stabilized, shear displacement δ was applied to the specimen at a constant rate of 0.01 in/min (0.0042 mm/s). This rate is more than twice the fastest rate in the Minkley and Mühlbauer (2007) study and orders of magnitude above the in situ rate, but it was the slowest rate the testing machine was capable of performing. The shear displacement application began with a load-unload-reload cycle in order to reduce unwanted compliance in the shear box assembly. The resulting stress magnitude during the initial loading was kept less than the yield stress of the specimen. Because the yield stress of an individual specimen was not known a priori, judgment was used to determine when to terminate the initial shear loading and begin unloading the specimen. The initial shear loading magnitude was chosen conservatively (approximately 20% of the normal nominal load), and the shear stress was unloaded until the stress-displacement curve became nonlinear. Shear loading was then resumed. Attempts were made to calculate the shear stiffness from the reloading response, but the results were deemed unreliable. The shear displacement rate was held constant until the residual strength of the specimen was achieved or until shear displacement was equal to 20% of the specimen diameter.

Application of shear displacement caused the top half of the specimen to protrude over the bottom half. This overhang led to a decrease in current cross-sectional area A available to resist the loads P and S. Treating the top and bottom halves of the specimen as perfect cylinders with diameter d, the current area was $A = ½ (\theta d^2 - \delta \sin\theta)$, where $\cos\theta = \delta/d$. The loss of cross-sectional area means the normal Cauchy stress P/A decreased by as much as 16% during the test, which is less than ideal, but likely a small error in the face of other uncertainties.

Upon attaining the residual strength or 20% shear displacement (whichever was achieved first), the shear load was unloaded and reloaded to measure the residual shear stiffness. The shear load was then removed, and the normal force was unloaded and reloaded to measure the residual normal stiffness. The normal force was then

removed from the specimen, and the shear boxes were separated. The failed surfaces were photographed.

After the intact specimen had been tested, the shear boxes were reset to their original position, and the test procedure was repeated on the failed specimen, this time at a greater normal stress. Additional information was gained regarding the residual deformation and strength characteristics with only a small labor increase by testing the already failed geologic interface. The effects of continued shearing and damage accumulation on the deformational properties could also be assessed. Once the residual test with the broken interface was completed and the boxes separated, a determination was made that further residual tests would provide no additional useful data.

Tests were performed on plain salt samples with no interface to evaluate the test setup for any possible bias. Samples that included a distinct interface, such as either a clay seam or a halite/anhydrite or polyhalite interface, were then tested. The testing room was kept at an ambient temperature of 68^{0}F (20.2^{0}C) during all tests.

3. RESULTS

This section begins with results from one specimen, followed by comparisons across the various specimen groups.

3.1. Specimen CARLSBAD/HALITE-CLAY/3/0.80

Figures 7 through 10 show the results of the tests on sample CARLSBAD/HALITE-CLAY/3/0.80, which was first tested as an intact sample at a normal stress of P/A_0 = 1500 psi (10.3 MPa), then retested at P/A_0 = 2400 psi (16.5 MPa). The sample was placed in the direct shear machine at an angle of 4^0, so that the interface was parallel to the shear displacement. Figure 7 shows the first test on the intact sample. The interface reached a maximum shear stress of S/A_0 = 1236 psi before beginning to yield, and eventually reached a residual shear stress of S/A_0 = 796 psi. Pre-test and post-test photographs of the intact sample are shown in Figure 8. Figure 9 shows the results of the subsequent residual test performed at P/A_0 = 2400 psi. The shear stress reached a residual value of 1013 psi. This value may be compared to the residual value obtained from the intact test performed for another sample at the same normal stress of 2400 psi; that sample, /6/0.80, reached a residual stress of S/A_0 = 1139 psi. In general, the residual stresses achieved in the residual tests were somewhat less than the residual stresses obtained from the intact tests at the same normal pressure. Finally, Figure 10 compares the post-test photographs from the intact and residual tests from the /3/0.80 sample. The additional test performed on the sample appears to have additionally ground down the surface of the interface, which may partially explain the lower residual stress than that for the test on the /6/0.80 sample.

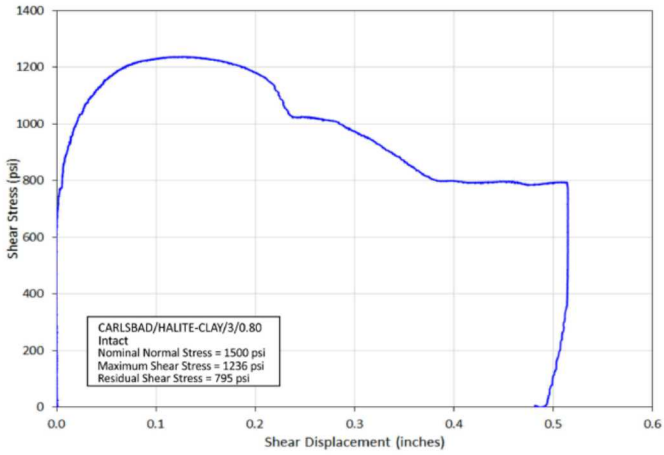

Fig. 7. Intact Test on Sample CARLSBAD/HALITE-CLAY/3/0.80 at Normal Pressure of 1500 psi.

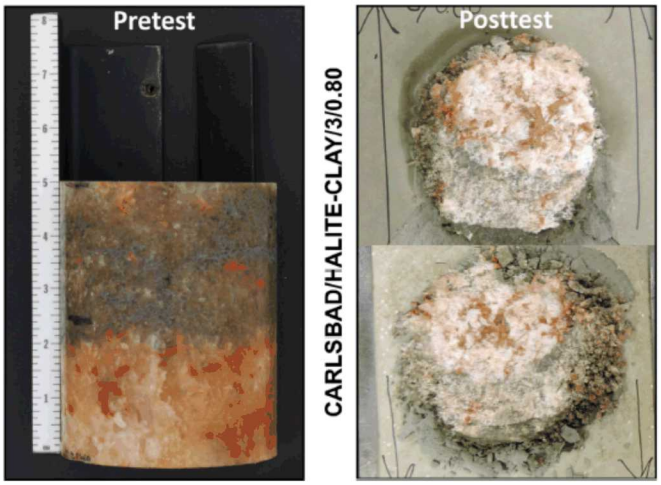

Fig. 8. Pre-test and Post-test Photos of Specimen CARLSBAD/HALITE-CLAY/3/0.80 after intact test.

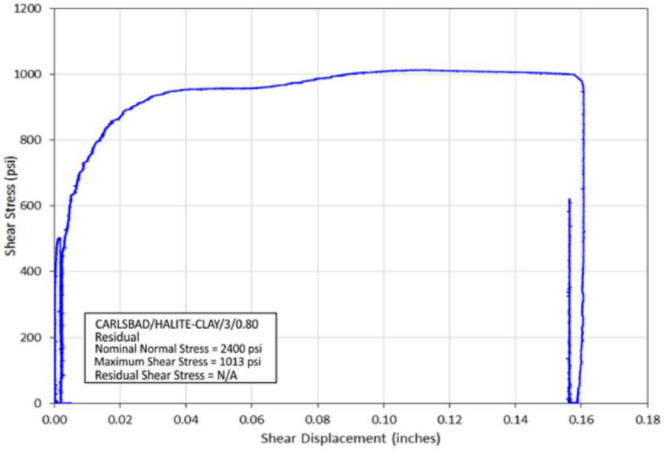

Fig. 9. Residual Test on Sample CARLSBAD/HALITE-CLAY/3/0.80 at Normal Pressure of 2400 psi.

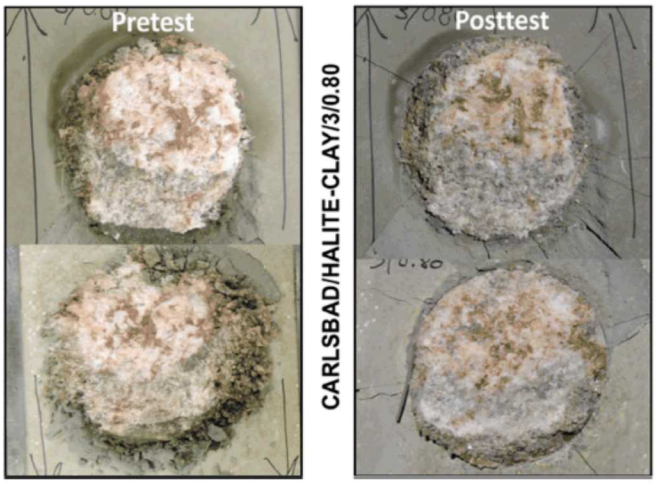

Fig. 10. Pre-test, Post-test photos from Residual Test of Sample CARLSBAD/HALITE-CLAY/3/0.80.

3.2. Comparisons

Table 2 lists the results of the tests, and Figures 11 through 16 show the shear stress S/A_0 versus shear displacement δ curves. All stresses in the table have units of psi, and stiffnesses are in psi/in.

Table 2. Test Results.

Specimen I.D.	Condition	Normal Stress (psi)	Max Shear Stress	Residual Shear Stress	Pre-Normal Stiffness	Post-Normal Stiffness
CANADA/HALITE-CLAY/506.07	Intact	300	398	255	41,275	36,407
CANADA/HALITE-CLAY/506.07	Residual	480	352	321	41,443	43,236
CANADA/HALITE-CLAY/506.07	Residual	600	396	—	43,584	48,357
CANADA/HALITE-CLAY/506.07	Residual	780	498	—	41,410	48,120
CANADA/HALITE-CLAY/507.28	Intact	500	454	401	41,333	39,887
CANADA/HALITE-CLAY/507.28	Residual	1,000	683	—	57,702	57,558
CANADA/HALITE-CLAY/507.28	Residual	1,500	952	—	63,736	71,146
CANADA/HALITE-CLAY/507.90	Intact	2,400	1,965	—	153,453	—
CANADA/HALITE-CLAY/507.90	Residual	2,400	1,612	—	119,772	394,324
CANADA/HALITE-CLAY/506.84	Intact	2,400	1,735	1,345	74,433	—
CARLSBAD/HALITE-CLAY/1/1.45	Intact	500	683	345	89,403	55,205
CARLSBAD/HALITE-CLAY/1/1.45	Residual	1,000	607	—	87,403	89,112
CARLSBAD/HALITE-CLAY/3/1.00	Intact	1,000	976	545	94,135	99,041
CARLSBAD/HALITE-CLAY/3/1.00	Residual	1,500	880	—	138,420	147,685
CARLSBAD/HALITE-CLAY/2/1.15	Intact	1,500	1,402	1,133	164,271	179,418
CARLSBAD/HALITE-CLAY/2/1.15	Residual	2,400	1,373	—	140,530	187,356
CARLSBAD/HALITE-CLAY/3/0.80	Intact	1,500	1,236	795	129,067	—
CARLSBAD/HALITE-CLAY/3/0.80	Residual	2,400	1,013	—	122,563	133,834
CARLSBAD/HALITE-CLAY/6/0.80	Intact	2,400	1,512	1,139	142,798	—
CARLSBAD/POLYHALITE-HALITE/5/0.64	Intact	500	676	433	157,308	176,694
CARLSBAD/POLYHALITE-HALITE/5/0.64	Residual	1,000	768	607	182,110	140,147
CARLSBAD/POLYHALITE-HALITE/1/0.10	Intact	500	379	—	118,760	69,356
CARLSBAD/POLYHALITE-HALITE/1/0.10	Residual	1,000	587	—	140,966	115,437
CARLSBAD/POLYHALITE-HALITE/6/1.92	Intact	1,000	1,322	616	121,395	116,254
CARLSBAD/POLYHALITE-HALITE/6/1.92	Residual	1,500	574	—	80,555	158,873
CARLSBAD/POLYHALITE-HALITE/4/0.64	Intact	1,000	1,090	561	152,833	114,999
CARLSBAD/POLYHALITE-HALITE/4/0.64	Residual	1,500	858	—	131,483	—
CARLSBAD/POLYHALITE-HALITE/4/1.59	Intact	1,500	1,358	583	240,304	131,111
CARLSBAD/POLYHALITE-HALITE/4/1.59	Residual	2,400	900	—	93,032	—
CARLSBAD/POLYHALITE-HALITE/3/1.59	Intact	2,400	1,639	970	138,188	99,536
CARLSBAD/MIXED-HALITE/1/1.76	Intact	500	667	314	124,281	72,592
CARLSBAD/MIXED-HALITE/1/1.76	Residual	1,000	617	—	101,085	117,734
CARLSBAD/MIXED-HALITE/3/1.00	Intact	500	730	333	76,088	68,095
CARLSBAD/MIXED-HALITE/3/1.00	Residual	1,000	595	—	142,181	99,392
CARLSBAD/MIXED-HALITE/2/1.76	Intact	1,000	1,323	747	113,402	175,694
CARLSBAD/MIXED-HALITE/2/1.76	Residual	1,500	1,173	—	106,341	—
CARLSBAD/MIXED-HALITE/4/1.76	Intact	1,500	1,626	1,018	166,915	122,277
CARLSBAD/MIXED-HALITE/4/1.76	Residual	2,400	1,628	—	177,872	—
CARLSBAD/MIXED-HALITE/5/1.76	Intact	2,400	1,960	1,323	163,491	—
CARLSBAD/PURE-HALITE/6/0.68	Intact	500	722	315	51,438	44,798
CARLSBAD/PURE-HALITE/6/0.68	Residual	1,000	552	—	77,895	94,034
CARLSBAD/PURE-HALITE/1/0.00	Intact	1,000	1,147	548	219,432	205,159
CARLSBAD/PURE-HALITE/1/0.00	Residual	1,500	879	—	115,270	150,543
CARLSBAD/PURE-HALITE/2/0.00	Intact	1,000	1,071	556	125,298	135,600
CARLSBAD/PURE-HALITE/2/0.00	Residual	1,500	619	—	117,424	150,683
CARLSBAD/PURE-HALITE/8/0.68	Intact	1,500	1,217	763	105,377	—
CARLSBAD/PURE-HALITE/8/0.68	Residual	2,400	914	—	133,758	175,719
CARLSBAD/PURE-HALITE/10/0.68	Intact	2,400	1,604	—	203,266	188,599
CARLSBAD/HALITE-ANHYDRITE/2/1.90	Intact	500	733	290	206,062	96,052
CARLSBAD/HALITE-ANHYDRITE/2/1.90	Residual	1,000	586	—	105,999	193,388
CARLSBAD/HALITE-ANHYDRITE/1/0.22	Intact	500	808	321	99,589	69,594
CARLSBAD/HALITE-ANHYDRITE/1/0.22	Residual	1,000	461	—	97,789	131,059
CARLSBAD/HALITE-ANHYDRITE/3/2.30	Intact	1,000	1,338	628	164,496	99,511
CARLSBAD/HALITE-ANHYDRITE/3/2.30	Residual	1,500	816	—	100,029	152,783
CARLSBAD/HALITE-ANHYDRITE/1/2.30	Intact	1,500	1,543	874	217,076	—
CARLSBAD/HALITE-ANHYDRITE/1/2.30	Residual	2,400	918	—	118,363	147,574
CARLSBAD/HALITE-ANHYDRITE/1/1.41	Intact	2,400	1,766	1,025	142,629	—

Some samples were stiffer in shear than the shear load transfer linkages of the testing machine. Once the shear strength of the specimen was exceeded, the shear linkages would suddenly release their strain energy, and the upper shear box essentially slingshot forward before self-arresting. The rapid change in shear displacement was captured by typically one or two data points collected at 5 hertz. The shear ram, which advanced at a constant rate, then had to rebuild the shear force until the broken interface began slipping. Consequently, the sharp increase of shear stress with little shear displacement in Figure 12 for the 500 and 1000 psi tests on halite-clay samples, for example, is an artifact of the contrast in stiffnesses between the shear linkages and the intact stiffness of the test specimens. The true post-peak shear stress-displacement behavior would be expected to be smooth and continuous.

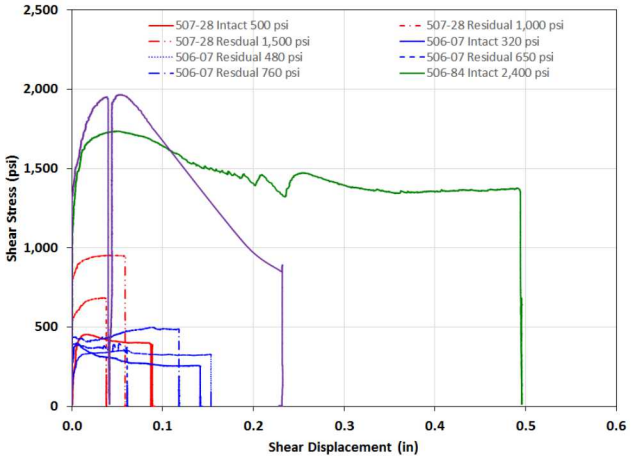

Fig. 11. Canada Halite-Clay Shear Stress Versus Shear Displacement.

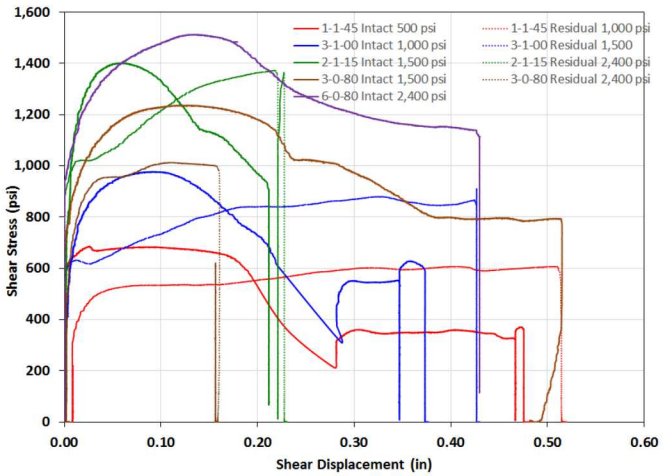

Fig. 12. Carlsbad Halite-Clay Shear Stress Versus Shear Displacement.

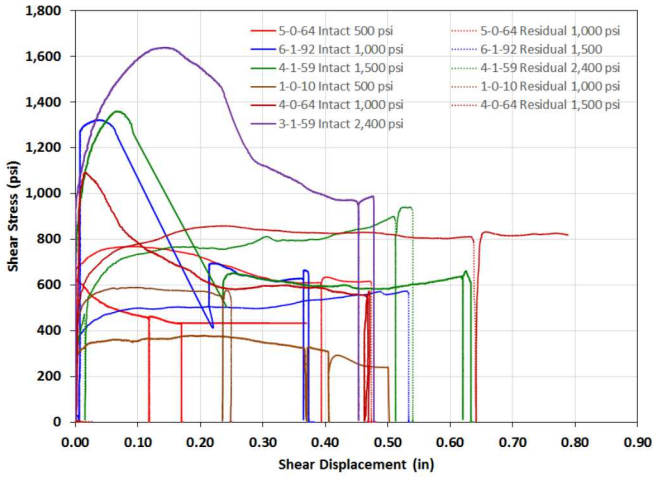

Fig. 13. Carlsbad Polyhalite-Halite Shear Stress Versus Shear Displacement.

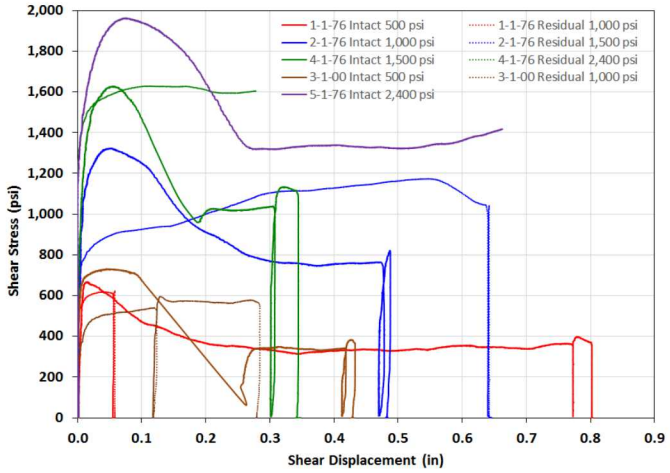

Fig. 14. Mixed Halite Shear Stress Versus Shear Displacement.

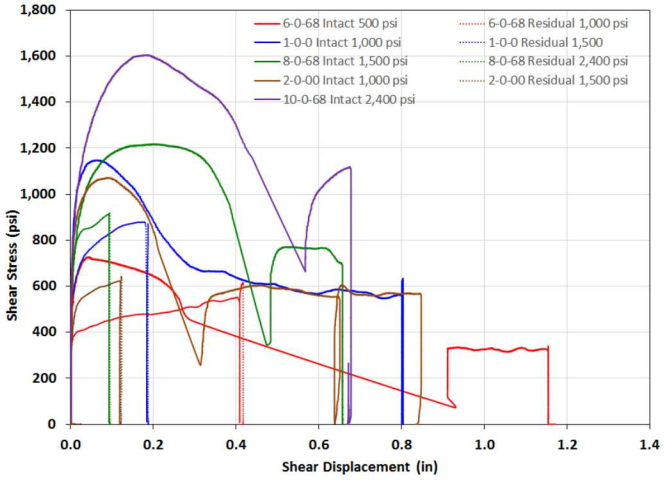

Fig. 15. Pure Halite Shear Stress Versus Shear Displacement.

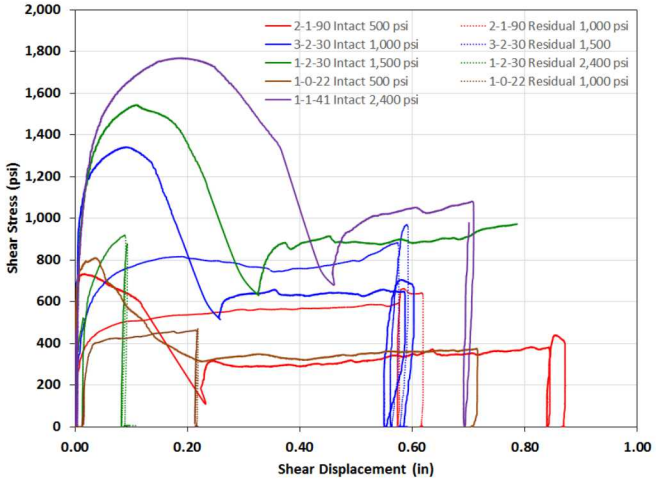

Fig. 16. Halite-Anhydrite Shear Stress Versus Shear Displacement.

The interface between the halite layer and the clay section is well-defined. The fractured interface revealed a significant intrusion of salt crystals through the interface, giving it a higher stiffness and greater fracture stress than was expected. This condition has been observed at other interfaces at the WIPP site (Holt and Powers, 2011), which is different than other less stiff clay interfaces there (Figure 2).

Figures 17 and 18 show the data fits for peak shear stress versus the normal stress for the intact and residual strengths, respectively. The stresses were calculated using the original cross-sectional area of the interface. The computed values for the cohesion (S_0) and friction angle (φ) are also shown on the plots. Data from the residual tests performed following each intact test are not plotted and were not included in the data fits because of the inconsistent behavior exhibited by the samples after the breaking of the interfaces. The simple Mohr-Coulomb fits reasonably capture each interface type. Notably, the cohesion strength is non-zero in all cases, suggesting the interfaces have a non-zero shear strength at zero normal stress.

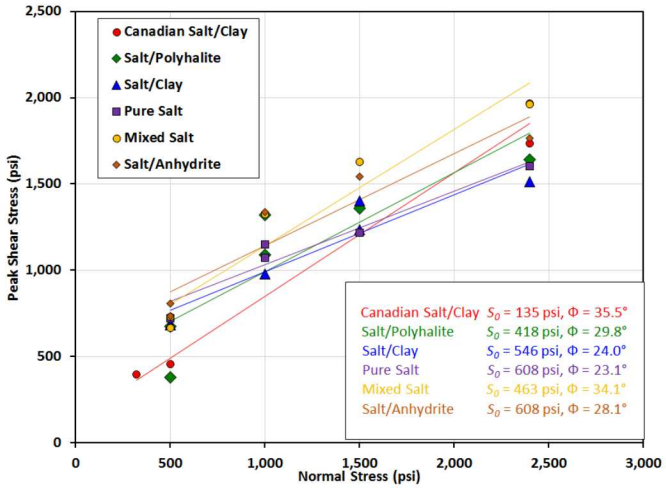

Fig. 17. Peak Shear Stress as a Function of Normal Stress.

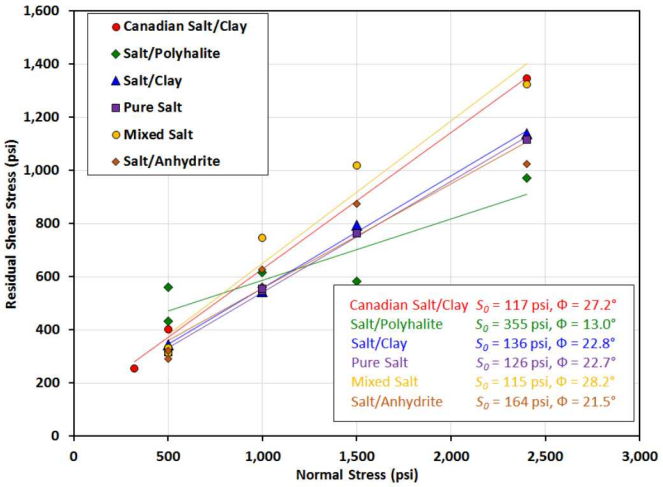

Fig. 18. Residual Shear Stress as a Function of Normal Stress.

The halite/clay interface is particularly of interest because of the presence of several clay seams in the region surrounding the WIPP site (see Figure 1). Given the prevalence of clay seam sliding at WIPP (see Figure 2), the clay interface was expected to have the lowest cohesion and friction angle, yet its behavior is more similar to that of pure salt. One potential reason for the large clay strengths was found upon examining the broken interfaces. The clay seams had salt crystals spanning the interface, such that the shear test was measuring the sliding of these crystals against one another with little clay to lubricate the interface.

The clay seams observed at WIPP typically have a thickness between 0.125-2 inches (3-50 mm) and are noticeably soft. Clay seam samples from depths closer to the WIPP horizon are currently difficult to obtain due to ventilation issues. For this reason, additional testing has been planned to include samples with artificially manufactured bentonite seams with thicknesses in the range described above. These tests should establish trends that will help interpret future tests on clay seam samples from the WIPP horizon.

4. CONCLUSIONS

Thirty samples were tested from six salt specimen types: two halite-clay contact types (one from Canada and one from Carlsbad), a polyhalite-halite contact, a mixed halite, a pure halite, and a halite-anhydrite contact. The tests ran according to procedure, and both maximum shear strength and residual shear strength were determined for each rock type. Regardless of the rock type (i.e., with or without contacts), specimens behaved and broke like solid rock. Each rock type reasonably conformed to Mohr-Coulomb behavior. The mixed halite consistently tested as the strongest sample group for peak shear stress and residual shear stress. The clay seams were expected to be the weakest interfaces, but the clay seam residual shear stresses were similar to the pure halite. Numerous halite crystals were found spanning the clay seams rather than a solid layer of clay. Future tests will be performed on artificially manufactured clay seams and clay seam samples from WIPP, if possible.

5. ACKNOWLEDGEMENTS

Sandia National Laboratories is a multimission laboratory managed and operated by National Technology and Engineering Solutions of Sandia, LLC., a wholly owned subsidiary of Honeywell International, Inc., for the U.S. Department of Energy's National Nuclear Security Administration under contract DE-NA0003525. This research is funded by WIPP programs administered by the Office of Environmental Management (EM) of the U.S. Department of Energy.

REFERENCES

1. Buchholz, S.A., 2019. Technical Letter Memorandum RSI/TLM-190, Direct Shear Testing of Bedded Interfaces and Clay Seams, RESPEC, Rapid City, South Dakota, January 11, 2019.

2. Hansen, F.D., Sobolik S.R., & Stauffer, P., 2016a. Intermediate Scale Testing Recommendation Report, FCRD-UFD-2016- 000030 Rev. 0, SAND2016-9041R, Sandia National Laboratories, Albuquerque, NM.

3. Hansen, F.D., Steininger, W., & Bollingerfehr W., 2016b. Proceedings of the 6th US/German Workshop on Salt Repository Research, Design, and Operation. FCRD-UFRD-2016-00069. SAND2016-0194R, Dresden, Germany, Sept. 2015. Sandia National Laboratories, Albuquerque, NM.

4. Hansen, F.D., Steininger, W., & Bollingerfehr, W., 2017. Proceedings of the 7th US/German Workshop on Salt Repository Research, Design, and Operation, SFWD-SFWST-2017-000008. SAND2017-1057R, Arlington, VA, Sept. 2016, Sandia National Laboratories, Albuquerque, NM.

5. Holt, R.M., and Powers, D.W., 2011. Synsedimentary dissolution pipes and the isolation of ancient bacteria and cellulose, Geological Society of America Bulletin, published online on 11 February 2011 as doi:10.1130/B30197.1.

6. Lüdeling, C., Salzer, K., Günther, R. -M., Hampel, A., Yildirim, S., Staudtmeister, K., Gährken, A., Stahlmann, J., Herchen, K., Lux, K.-H., Reedlunn, B., Sobolik, S., Hansen, F.D. & Buchholz, S.A. (2018). WEIMOS: Joint Project on further development and qualification of the rock mechanical modeling for the final HLW disposal in rock salt. Overview and first results on tensile stress modeling. Proceedings of the 9th Conference on the Mechanical Behavior of Salt (Saltmech IX), 12-14 Sept. 2018, Hannover, Germany. Eds.: S. Fahland, J. Hammer, F.D. Hansen, S. Heusermann, K.-H. Lux & W. Minkley,

published by BGR Hannover, ISBN 978-3-9814108-6-0, pp. 459-477.

7. Minkley, W. & M Mühlbauer, J., 2007. Constitutive Models to Describe the Mechanical Behavior of Salt Rocks and the Imbedded Weakened Planes. Wallner, M., K-H Lux, W. Minkley, H.R. Hardy, eds. The Mechanical Behavior of Salt: Understanding of THMC Processes in Salt. Taylor & Francis/Balkema, Leiden, The Netherlands.

8. Munson, D.E. & Matalucci, R.V., 1983. Planning, Developing, and Fielding of Thermal/Structural Interactions in situ Tests for the Waste Isolation Pilot Plant (WIPP). SAND83-2048. Sandia National Laboratories, Albuquerque NM.

9. Sobolik, S., 2017. Experimental Investigation of WIPP Salt Samples and Clay Seams. TP 17-03 Rev. 0. Sandia